

FIGURE 4. Slit-lamp photographs of cases 4, 5, and 6 (A, D, G). HRT II-RCM image of the area of the infiltrates of case 4, 5, and 6 showing highly reflective, hyphae-like, interlocking and branching, white lines (B, E, H). Light microscopic observation of smear with Giemsa staining of case 4, 5, and 6 showed filamentous fungi (C, F, I). The depth at which all of the HRT II-RCM images were taken is indicated on the bottom right corner.

However, it is not easy to determine the indications for surgical debridement by slit-lamp microscopy because slit-lamp microscopy may not be able to differentiate the morphology of ulcerated lesion and infiltrates. In case 3, the HRT II-RCM examination clearly revealed the mass of hyphae in the necrotic tissue in the corneal ulcerated lesion, suggesting that surgical debridement was necessary. We performed surgical

debridement twice under HRT II-RCM monitoring, and these procedures resulted in a complete epithelial healing along with the decrease in the density of hyphae.

In summary, our findings showed that the HRT II-RCM will help in the diagnosis of FK and its noninvasiveness allows repeated assessments that should make this instrument a useful tool for judging the effectiveness of the treatments.

REFERENCES

1. Iyer SA, Tuli SS, Wagoner RC. Fungal keratitis: emerging trends and treatment outcomes. *Eye Contact Lens*. 2006;32:267–271.
2. Shukla PK, Kumar M, Keshava GB. Mycotic keratitis: an overview of diagnosis and therapy. *Mycoses*. 2008;51:183–199.
3. Thomas PA. Fungal infections of the cornea. *Eye*. 2003;17:852–862.
4. Florakis GJ, Moazami G, Schubert H, et al. Scanning slit confocal microscopy of fungal keratitis. *Arch Ophthalmol*. 1997;115:1461–1463.
5. Winchester K, Mathers WD, Sutphin JE. Diagnosis of *Aspergillus* keratitis in vivo with confocal microscopy. *Cornea*. 1997;16:27–31.
6. Das S, Samant M, Garg P, et al. Role of confocal microscopy in deep fungal keratitis. *Cornea*. 2009;28:11–13.
7. Kanavi MR, Javadi M, Yazdani S, et al. Sensitivity and specificity of confocal scan in the diagnosis of infectious keratitis. *Cornea*. 2007;26:782–786.
8. Brasnu E, Bourcier T, Dupas B, et al. In vivo confocal microscopy in fungal keratitis. *Br J Ophthalmol*. 2007;91:588–591.
9. Bourcier T, Dupas B, Borderie V, et al. Heidelberg retina tomograph II findings of *Acanthamoeba* keratitis. *Ocul Immunol Inflamm*. 2005;13:487–492.
10. Shiraishi A, Hara Y, Takahashi M, et al. Demonstration of “owl’s eye” morphology by confocal microscopy in a patient with presumed cytomegalovirus corneal endotheliitis. *Am J Ophthalmol*. 2007;143:715–717.
11. Kobayashi A, Ishibashi Y, Oikawa Y, et al. In vivo and ex vivo laser confocal microscopy findings in patients with early-stage acanthamoeba keratitis. *Cornea*. 2008;27:439–445.
12. World Medical Association declaration of Helsinki. Recommendations guiding physicians in biomedical research involving human subjects. *JAMA*. 1997;277:925–926.
13. Miller WL, Giannoni AG, Perrigin J. A case of fungal keratitis: a clinical and in vivo confocal microscopy assessment. *Cont Lens Anterior Eye*. 2008;31:201–206.
14. Shi W, Li S, Liu M, et al. Antifungal chemotherapy for fungal keratitis guided by in vivo confocal microscopy. *Graefes Arch Clin Exp Ophthalmol*. 2008;246:581–586.

Connective Tissue Growth Factor Cooperates with Fibronectin in Enhancing Attachment and Migration of Corneal Epithelial Cells

Koji Sugioka,¹ Koji Yoshida,² Aya Kodama,¹ Hiroshi Mishima,³ Kosuke Abe,¹ Hiroshi Munakata² and Yoshikazu Shimomura¹

¹Department of Ophthalmology, Kinki University School of Medicine, Osaka-Sayama, Japan

²Department of Biochemistry, Kinki University School of Medicine, Osaka-Sayama, Japan

³Department of Ophthalmology, Kinki University School of Medicine Nara, Nara, Japan

Corneal wound healing is a complex process involving the integrated actions of various growth factors, cytokines and extracellular matrix produced by corneal cells and inflammatory cells. Connective tissue growth factor (CTGF) has been linked to wound healing, and fibronectin (FN) is a major component of the extracellular matrix. However, the functions of CTGF and FN in corneal epithelial cells are not well understood. We therefore investigated the coordinated function of CTGF and FN in the attachment and migration of corneal epithelial cells. Treatment of human corneal epithelial cells (HCECs) with transforming growth factor (TGF) β 1 up-regulated the expression of CTGF, but did not noticeably affect FN expression, as judged by immunoblot analysis of cell lysates. In contrast, the amount of FN accumulated in the cultured media was increased in a time-dependent manner, but CTGF was undetectable in the cultured media. The expression level of FN was decreased by the knockdown of CTGF expression with a specific short hairpin RNA, indicating that CTGF acts as an upstream mediator of FN expression. CTGF augmented the FN-mediated increase in the attachment of HCEC by about twofold, although CTGF alone did not influence the attachment. Moreover, the migration assay with rabbit corneal blocks revealed that CTGF (390 nM) alone or in combination of FN (10 μ g/mL) promoted corneal epithelial migration; the mean migration distances of control, CTGF, and CTGF + FN were 272, 325, and 626, μ m, respectively. In conclusion, CTGF cooperates with FN in enhancing the attachment and migration of corneal epithelial cells.

Keywords: connective tissue growth factor; fibronectin; corneal epithelial cells; wound healing; migration
Tohoku J. Exp. Med., 2010, 222 (1), 45-50. © 2010 Tohoku University Medical Press

The cornea is directly challenged to the exterior environments. Therefore, corneal epithelium plays a pivotal role as a barrier to keep the integrity of the ocular surface. When epithelial defects occur on the cornea, rapid re-epithelialization is critical in order to prevent invasion of pathogens into the corneal stroma. The corneal epithelium maintains its homeostasis and physiological characteristics by repeating a cycle of proliferation, migration and surficial cell loss (Thoft and Friend 1983). Smooth corneal epithelial cell migration plays a central role in corneal epithelial wound healing; various growth factors, cytokines and extracellular matrices are all necessary for this cell migration (Wilson et al. 1992; Li and Tseng 1995). Furthermore, stromal-epithelial interactions occur during corneal wound healing (Wilson et al. 1999) and activated keratocytes undergo myofibroblastic transformation (Jester et al. 1995; Funderburgh et al. 2003).

Connective tissue growth factor (CTGF) is a down-

stream mediator of transforming growth factor (TGF)- β and is found in abundance in the lacrimal fluid (Grotendorst 1997). CTGF is thought to play a role in maintenance of fibrosis (Bradham et al. 1991). It was reported that CTGF expression is increased in fibrotic diseases of the lung (Allen et al. 1999), kidney (Ito et al. 1998), and skin (Igarashi et al. 1995); this mediator may be involved in the storage of the extracellular matrix. CTGF also exerts effects on cell attachment and migration (Fan et al. 2000). In the cornea, CTGF promotes transdifferentiation of the corneal fibroblast into the myofibroblast, resulting in excess production of collagen and fibronectin (FN). CTGF is also involved in the wound healing process of the corneal stroma (Folger et al. 2001; Blalock et al. 2003; Garrett et al. 2004). One of the reasons why CTGF has so many functions may be due to its binding to other cytokines and the extracellular matrix to modulate their actions (Frazier et al. 1996).

We reported that CTGF binds to FN (Yoshida and

Received May 26, 2010; revision accepted for publication August 9, 2010. doi: 10.1620/tjem.222.45

Correspondence: Koji Sugioka, M.D., Ph.D., Department of Ophthalmology, Kinki University School of Medicine, 377-2 Ohno-Higashi, Osaka-Sayama city, Osaka 589-8511, Japan.
e-mail: sugioka@ganka.med.kindai.ac.jp

Munakata 2007). Although the action of CTGF on the corneal epithelium is not well known, it has been shown that FN promotes corneal epithelial cell migration in culture (Watanabe et al. 1987) as well as in vivo (Nishida et al. 1983b). Therefore, we examined the role of CTGF in corneal epithelial wound healing using cultured corneal epithelial cells and focusing on the interaction between FN and CTGF. We also used an organ culture method to investigate corneal epithelial cell migration.

Materials and Methods

Cell Culture

A human corneal epithelial cell (HCEC) line established using a simian virus 40 (SV40)-adenovirus recombinant vector was kindly provided by K. Araki-Sasaki. The cells were maintained in Dulbecco's modified Eagle's medium (DMEM)/F12 (1:1) (Gibco; Grand Island, NY, USA) containing 10% fetal bovine serum (FBS) (Gibco) at 37°C under humidified 5% CO₂ and 95% air.

Animals

Female albino rabbits weighting 2 to 3 kg were obtained from Hokusetsu Sangyo (Settsu, Osaka, Japan). This study was performed in compliance with the Rules and Regulations of the Animal Care and Use Committee, Kinki University School of Medicine, and followed the Guide for the Care and Use of Laboratory Animals, Kinki University School of Medicine.

Proteins

Human plasma fibronectin was purchased from Sigma-Aldrich (St. Louis, MO, USA). TGF- β 1 was purchased from R & D Systems (Minneapolis, MN, USA). The recombinant His-tagged human CTGF was purchased from Biovendor Laboratory Medicine, Inc. (Brno, Czech Republic).

Antibodies

The goat anti-human CTGF polyclonal antibody was purchased from R & D Systems. The rabbit anti-human FN polyclonal antibody and anti-human β -actin monoclonal antibody were purchased from Sigma-Aldrich. Horseradish peroxidase-conjugated donkey anti-rabbit and sheep anti-mouse IgG antibodies were purchased from GE Healthcare Bio-Sciences (Piscataway, NJ, USA). Horseradish peroxidase-conjugated rabbit anti-goat IgG antibody was purchased from MBL (Nagoya, Japan). For the cell attachment assay, the mouse IgG anti-human FN was purchased from Takara Bio Inc. (Shiga, Japan) and normal mouse IgG was purchased from Sigma-Aldrich.

Plasmids and Transfection

Four independent short hairpin RNA (shRNA) constructs which were targeting four different exons of CTGF and one control plasmid were purchased from SABiosciences Corporation (Frederick, MD, USA). The sequences included CTGFshRNA1:5'-CCAGACCAACTATGATTAGA-3'; CTGFshRNA2:5'-AGACATACCGAGCTAAATTCT-3'; CTGFshRNA3:5'-TACCGACTGGAAGACACGTTT-3'; CTGFshRNA4:5'-TGACCTGGAAGAGAACATTAA-3'; and shRNA:5'-TGACCTGGAAGAGAACATTAA-3' (negative control). HCECs were transfected with CTGFshRNA and control plasmids using lipofectamine 2000 transfection reagent (Invitrogen; Carlsbad, CA, USA) following the manufacturer's instructions.

Briefly, HCEC-coated 12-well plates were grown to 95% confluence. Four microliters of lipofectamine 2000 reagent was diluted in 96 μ L Opti-MEM medium (Invitrogen) and then mixed with 100 μ L Opti-MEM which included 1.6 μ g of shRNA plasmids. After incubating at 37°C for 4 hours, the medium was changed to DMEM containing 10% FBS and the plates were incubated for 48 hours under the same conditions.

Immunoblot Analysis

To examine the effects on CTGF and FN expression in HCECs by stimulating TGF- β 1, HCECs were cultured in DMEM containing 10% FBS. Prior to stimulation, cells were rendered quiescent by being maintained in serum-starved conditions for 24 hours. They were subsequently treated with 10 ng/mL of TGF- β 1 for up to 72 hours. Mean TGF- β 1 concentration in tear fluid is approximately 10–20 ng/mL (Gupta et al. 1996); therefore, TGF- β 1 concentration of 10 ng/mL was used in this experiment. The cell lysates and the conditioned media were collected at 0, 12, 24, 48, and 72 hours after TGF- β 1 stimulation. To investigate the role of CTGF in FN expression, HCECs transfected with CTGFshRNA were prepared as stated above. Cell lysates were prepared as described previously (Yoshida and Munakata 2007). The lysates were examined by Western blot using antibodies against polyclonal goat anti-human CTGF, polyclonal rabbit anti-human FN, monoclonal anti- β -actin and peroxidase-linked secondary antibodies. The immunoblotted membrane was developed using an enzyme-linked chemiluminescence (ECL) kit (GE Healthcare Bio-Sciences) according to the manufacturer's instructions.

Cell Attachment Assay

Two experiments were performed to examine the interaction between CTGF and FN. In the first experiment, 1% bovine serum albumin (BSA) (Roche Diagnostics, Switzerland), CTGF, FN or CTGF+FN were added to the media and incubated for 2 hours. After the 2-hour incubation, HCECs in the wells (1,000 cells/well) were incubated in the treated media at 37°C for 45 minutes. In the second experiment, 100 μ L of HCEC suspension (1,000 cells/well) was placed in plates with FN-coated or uncoated wells. CTGF, CTGF + goat IgG anti-human FN, CTGF + normal goat IgG or 1% BSA, 1% BSA + mouse IgG anti-human FN, or 1% BSA + normal mouse IgG were added to the medium to investigate FN-dependant mechanisms. The cells were fixed and stained with 1% crystal violet in 95% ethanol, and the attached cells were counted under a phase-contrast microscope. Quadruplicate samples per treatment were tested and their mean average was obtained. Data were expressed as mean \pm standard error of the mean (SEM) of the number of attached cells/well in three independent experiments.

Corneal Epithelial Migration Assay

The distance of rabbit corneal epithelial cell migration in culture was measured by a previously described method (Nishida et al. 1983a). Briefly, rabbits were anesthetized with an intravenous injection of sodium pentobarbital (25 mg/kg body weight) and both eyes were enucleated. The sclerocorneal rim was excised, and the corneas were removed and then cut into small blocks with a razor blade. Six blocks (approximately 2 mm \times 4 mm) were obtained from each cornea. The blocks were placed in 24-well culture plates and incubated for 24 hours in the medium containing either 1) CTGF at concentrations of 0, 390 nM or 3.9 μ M, or 2) CTGF at the same concentration

plus FN (10 $\mu\text{g}/\text{mL}$). Multiple blocks from the same cornea were used in each experiment. The blocks were paraffin-embedded. Four thin sections (3 μm thick) were cut at 200 μm intervals from each block and stained using hematoxylin-eosin. The length of the path of epithelial migration down both sides of each section was measured on the micrographs. Results obtained from the four sections of each side of each block were averaged as one measurement. Each value is the average \pm SEM in three independent experiments.

Statistical Analysis

Statistical comparisons between two groups were performed by unpaired Student's *t*-test. ANOVA was used to compare three or more conditions with post hoc comparisons using the Tukey-Kramer procedure; *p* values < 0.05 were considered significant. Significant differences between groups are noted by *, † and ‡. Single symbol stands for *p* < 0.05, two symbols, for *p* < 0.01.

Results

Effects of TGF- β 1 on expression of CTGF and FN in HCECs

TGF- β 1 is known as a potent stimulator for connective tissue formation during wound repair and abundantly present in human tear fluid. It is also known that TGF- β 1 regulates CTGF expression and stimulates FN synthesis. Therefore, we examined whether the addition of TGF- β 1 promotes the expression levels of CTGF and FN in HCECs. The expression levels of CTGF and FN were analyzed in HCECs treated with TGF- β 1 by Western blotting. As shown in Fig. 1, treatment with TGF- β 1 up-regulated CTGF expression at 48 and 72 hours, but did not affect FN expression at any time point up to 72 hours in cell lysates. Western blot analysis of the conditioned media was used to characterize CTGF and FN released to the conditioned medium. The amount of FN accumulated in the cultured media was increased in a time-dependent manner (Fig. 1), but we could not detect CTGF in the cultured media at any time point up to 72 hours (data not shown).

Suppression of FN expression with knockdown of CTGF expression

Because CTGF is involved in wound healing and fibrosis, CTGF may play a role in FN synthesis. To test this hypothesis, CTGF-specific shRNAs were introduced into HCECs and their effects on the expression of CTGF and FN were examined. As shown in Fig. 2, CTGF-specific shRNA1 and shRNA2 suppressed CTGF and FN expression in HCECs. The negative control of shRNA and lipofectamine 2000 solution had no inhibitory effects on either CTGF or FN production. CTGF-specific shRNA3 and shRNA4 had weak inhibitory effects on the expression of CTGF and FN compared with shRNA1 and shRNA2.

Cell Attachment Assay

Although FN (10 $\mu\text{g}/\text{mL}$) itself facilitated the HCEC attachment to wells much more than control (1% BSA), CTGF significantly increased the number of HCECs

attached in the presence of FN in the conditioned media compared with FN alone. However, CTGF alone had little effect on cell attachment (Fig. 3). There were no significant differences in the number of attachment cells between the CTGF concentration of 1.3 μM and 3.9 μM .

To further characterize the interaction between the CTGF and FN, FN-coated wells were prepared and the effects of CTGF, BSA or anti-FN antibody on cell attachment were examined. The media containing CTGF significantly promoted the attachment of HCECs compared with control (BSA), whereas anti-FN antibody completely inhibited CTGF-stimulated cellular adhesion to FN in comparison with control (IgG antibody) (Fig. 4). These results suggest that CTGF-stimulated cellular adhesion would be a FN-dependant pathway.

The Effect of CTGF in the Presence or Absence of FN on Corneal Epithelial Cell Migration

Epithelial cell migration over cultured corneal blocks showed that CTGF alone stimulated epithelial cell migration in a dose-dependent manner (Fig. 5). Mean values of control, CTGF (390 nM), CTGF (390 nM) + FN, and CTGF (3.9 μM) were 272, 325, 626, and 720 μm , respectively. CTGF (390 nM) plus FN (10 $\mu\text{g}/\text{mL}$) promoted significantly greater epithelial cell migration compared to CTGF alone (Fig. 5). When the CTGF concentration in the media was 3.9 μM , no significant difference in migration distance was seen between CTGF plus FN and CTGF alone (Fig. 5).

Discussion

This report documents the interaction between CTGF and FN in corneal epithelial adhesion and cell migration. Little is known about the effects of CTGF on corneal epithelial cells. Recently, Secker et al. (2008) demonstrated that CTGF regulates corneal re-epithelialization stimulated by TGF- β 1. Our results concur with their report that CTGF promotes corneal epithelial migration and expand on their findings by demonstrating that CTGF promoted corneal epithelial cell adhesion and migration in the presence of FN, even in the absence of TGF- β 1.

To the best of our knowledge, there are no reports where protein level fluctuation of FN stimulated by TGF- β 1 in cultured human corneal epithelial cells was investigated, although there are many papers reporting that TGF- β 1 stimulates an increase in the expression of FN in the corneal fibroblasts (Ohji et al. 1993; Sharma et al. 2009). As shown in Fig. 1, TGF- β 1 promoted CTGF expression, but did not affect FN production in the cell lysates. However, Western blot analysis of the conditioned media from HCECs treated with TGF- β 1 showed that the amount of FN released by HCECs were increased in a time-dependent manner. This is probably that FN is constitutively expressed in the corneal epithelial cells and the accumulation of secreted FN was increased in the media. On the other hand, CTGF could be detected in the cell lysates, while could not be detected in the supernatant of the cultured media (Fig. 1). This is prob-

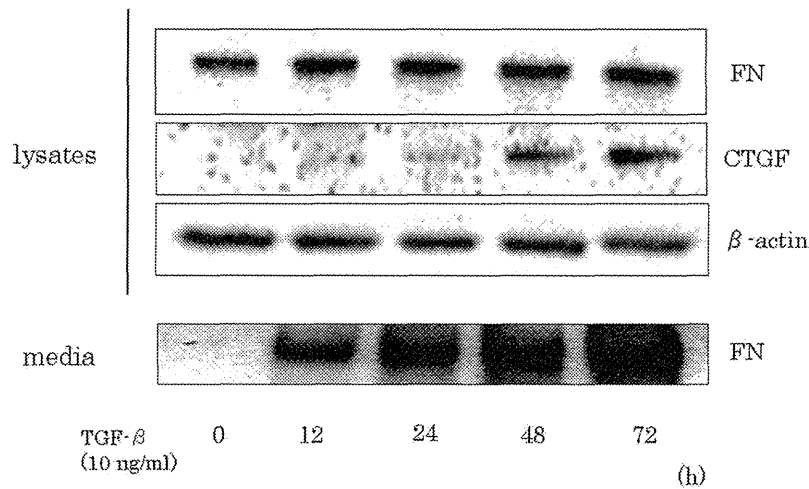


Fig. 1. Western blot analysis of FN, CTGF and β -actin in HCECs.

HCECs were incubated with 10 ng/mL of TGF- β 1. At the indicated time, cells were recovered and lysed. The cell lysates and conditioned media were separated in a polyacrylamide gel. After SDS-PAGE, the proteins were transferred onto PVDF membrane, and probed with anti-FN, CTGF or β -actin antibody. β -actin was used as a loading control.

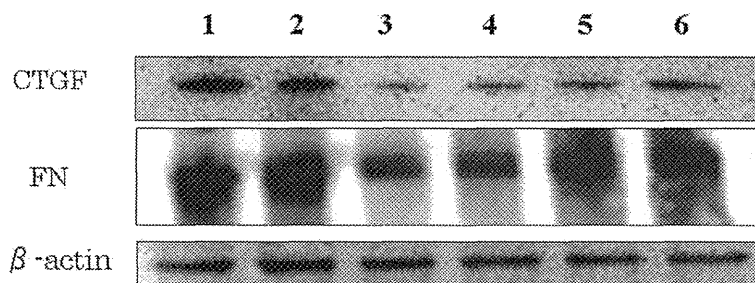


Fig. 2. Effects of shRNA on the production of CTGF and FN in HCECs at 48 hours post-transfection.

Whole cell lysates of each sample were assayed by Western blot analysis. β -actin was used as a loading control. Lane 1: lipofectamine 2000; Lane 2: negative control shRNA; Lane 3: CTGF shRNA1; Lane 4: CTGF shRNA2; Lane 5: CTGF shRNA3; Lane 6: shRNA4.

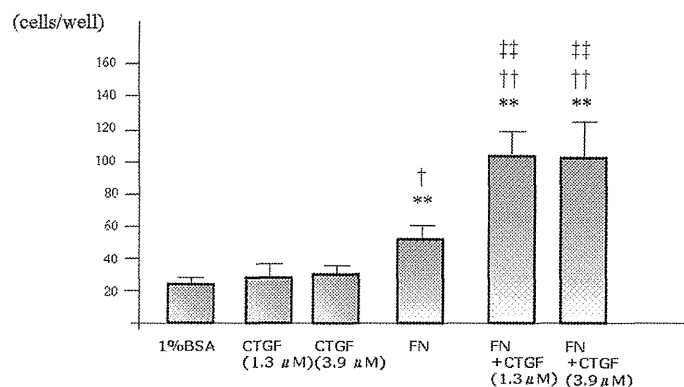


Fig. 3. Enhancement of cell adhesion by CTGF and FN.

Cells (1000 cells/well) were incubated with 1% BSA, CTGF (1.3 μ M, 3.9 μ M), FN (10 μ g/mL), or CTGF (1.3 μ M, 3.9 μ M) + FN (10 μ g/mL) for 45 minutes. After 45-minute incubation, adhesive cells were counted. Data were the mean \pm SEM of the number of attached cells/well in three independent experiments. Significant difference compared with the * 1% BSA group, † CTGF group (1.3 μ M), ‡ FN group. Single symbol stands for $p < 0.05$; two symbols, for $p < 0.01$.

ably because the amount of secreted CTGF was too minute to be detected. The coordination between CTGF and FN expression in cell lysates and media was not observed. One

interpretation for these results is FN may be secreted into the media much more than CTGF. Further study is required to clarify the precise mechanism of the phenomena.

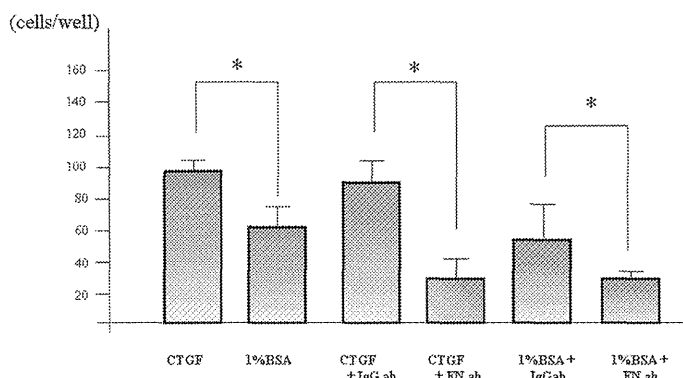


Fig. 4. The inhibitory effects of anti-FN antibody on CTGF-induced cell adhesion.

Wells were coated with FN ($2 \mu\text{g}/\text{mL}$) and incubated with 1,000 cells in the presence of CTGF or 1% BSA. CTGF facilitated cell attachment on FN-coated well ($*p < 0.05$). Cell adhesion to FN-coated wells was compared after adding anti-FN antibody or control IgG antibody along with CTGF ($1.3 \mu\text{M}$) or 1% BSA. Cells (1,000 cells/well) were incubated for 45 minutes. After 45-minute incubation, adhesive cells were counted. Enhancement of cell adhesion to FN by CTGF was inhibited by anti-FN antibody. Data were the mean \pm SEM of the number of attached cells/well in three independent experiments ($*p < 0.05$).

Secondly, we synthesized four CTGF-specific shRNAs and transfected them into corneal epithelial cells to examine their effects on the expression of CTGF and FN. Western blot analysis showed that two of the four constructed shRNAs strongly inhibited CTGF protein production, but the other shRNAs had weak inhibitory effects. The reason for the different results observed with these shRNAs might be due to a position effect. In the present study, the transfected cells which suppressed CTGF production also inhibited FN production and CTGF clearly regulated the expression of FN as shown in Fig. 2. Therefore, we suspect that FN functions downstream of CTGF.

Based on the results of our cell attachment assay, we indicated that CTGF bound to FN would have synergistic effects in promoting corneal epithelial cell adhesion. To our knowledge, there is no report which has investigated the adhesive function of CTGF to corneal epithelial cells, although there are some reports that demonstrated that CTGF enhanced cell adhesion of other types of cells to FN (such as stellate cells, sinusoidal endothelial cells, and chondrocytes) (Hoshijima et al. 2006; Pi et al. 2008).

Moreover, in our organ culture model, we have demonstrated that the interaction of CTGF and FN promoted corneal epithelial migration significantly when compared to FN alone at the CTGF concentration of 390 nM. However, CTGF (at $3.9 \mu\text{M}$) alone had almost the same level of corneal epithelial migration promotion as did a combination of CTGF and FN. As to this fact, we propose that at the concentration of $3.9 \mu\text{M}$, even with CTGF alone, the maximum corneal epithelial migration was achieved; however, it is possible that other factors besides FN are involved in promotion of CTGF-induced corneal epithelial cell migration.

The present study is limited to in vitro and organ culture experiments, with no in vivo investigations. In vivo, TGF- β 1 is abundantly present on the surface of the eye, as are other factors suppressing CTGF, which leads to more

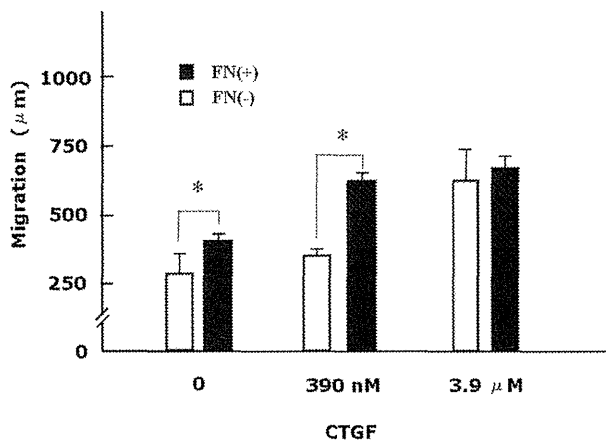


Fig. 5. Effects of CTGF and FN on corneal epithelial cell migration.

Corneal blocks were cultured for 24 hours with various concentrations of CTGF either with or without FN ($10 \mu\text{g}/\text{mL}$). The length of the path of epithelial migration was measured on the micrographs. With the concentration of CTGF at 390 nM, CTGF plus FN significantly promoted epithelial cell migration than CTGF alone. However, the $3.9 \mu\text{M}$ concentration of CTGF alone promoted migration of corneal epithelial cells without the presence of FN. Each value is the average \pm SEM in three independent experiments ($*p < 0.05$).

complex regulation of CTGF. The results of our cell attachment assay showed no effects on cell attachment with CTGF alone, and the effect of CTGF on the cell attachment was FN-dependent. In the organ culture model, however, the $3.9 \mu\text{M}$ concentration of CTGF alone promoted migration of corneal epithelial cells independent of FN.

Our study has an advantage in that we have proven coordination of CTGF and FN in the adhesion and migration of corneal epithelial cells. We anticipate that we may be able to apply our results clinically by controlling CTGF,

which has a close relationship with TGF- β 1 and FN, for treatment of some intractable corneal epithelial diseases.

Acknowledgments

This work was supported partly by grants from Osaka Eye Bank, The Osaka Medical Research Foundation for Incurable Diseases and Grant-in-Aid for Scientific Research (C) (20592111).

References

- Allen, J.T., Knight, R.A., Bloor, C.A. & Spiteri, M.A. (1999) Enhanced insulin-like growth factor binding protein-related protein 2 (Connective tissue growth factor) expression in patients with idiopathic pulmonary fibrosis and pulmonary sarcoidosis. *Am. J. Respir. Cell Mol. Biol.*, **21**, 693-700.
- Blalock, T.D., Duncan, M.R., Varela, J.C., Goldstein, M.H., Tuli, S.S., Grotendorst, G.R. & Schultz, G.S. (2003) Connective tissue growth factor expression and action in human corneal fibroblast cultures and rat corneas after photorefractive keratectomy. *Invest. Ophthalmol. Vis. Sci.*, **44**, 1879-1887.
- Bradham, D.M., Igarashi, A., Potter, R.L. & Grotendorst, G.R. (1991) Connective tissue growth factor: a cysteine-rich mitogen secreted by human vascular endothelial cells is related to the SRC-induced immediate early gene product CEF-10. *J. Cell Biol.*, **114**, 1285-1294.
- Fan, W.H., Pech, M. & Karnovsky, M.J. (2000) Connective tissue growth factor (CTGF) stimulates vascular smooth muscle cell growth and migration in vitro. *Eur. J. Cell Biol.*, **79**, 915-923.
- Folger, P.A., Zekaria, D., Grotendorst, G. & Masur, S.K. (2001) Transforming growth factor-beta-stimulated connective tissue growth factor expression during corneal myofibroblast differentiation. *Invest. Ophthalmol. Vis. Sci.*, **42**, 2534-2541.
- Frazier, K., Williams, S., Kothapalli, D., Klapper, H. & Grotendorst, G.R. (1996) Stimulation of fibroblast cell growth, matrix production, and granulation tissue formation by connective tissue growth factor. *J. Invest. Dermatol.*, **107**, 404-411.
- Funderburgh, J.L., Mann, M.M. & Funderburgh, M.L. (2003) Keratocyte phenotype mediates proteoglycan structure: a role for fibroblasts in corneal fibrosis. *J. Biol. Chem.*, **278**, 45629-45637.
- Garrett, Q., Khaw, P.T., Blalock, T.D., Schultz, G.S., Grotendorst, G.R. & Daniels, J.T. (2004) Involvement of CTGF in TGF-beta1-stimulation of myofibroblast differentiation and collagen matrix contraction in the presence of mechanical stress. *Invest. Ophthalmol. Vis. Sci.*, **45**, 1109-1116.
- Grotendorst, G.R. (1997) Connective tissue growth factor: a mediator of TGF-beta action on fibroblasts. *Cytokine Growth Factor Rev.*, **8**, 171-179.
- Gupta, A., Monroy, D., Ji, Z., Yoshino, K., Huang, A. & Pflugfelder, S.C. (1996) Transforming growth factor beta-1 and beta-2 in human tear fluid. *Curr. Eye Res.*, **15**, 605-614.
- Hoshijima, M., Hattori, T., Inoue, M., Araki, D., Hanagata, H., Miyauchi, A. & Takigawa, M. (2006) CT domain of CCN2/CTGF directly interacts with fibronectin and enhances cell adhesion of chondrocytes through integrin alpha5beta1. *FEBS Lett.*, **580**, 1376-1382.
- Igarashi, A., Nashiro, K., Kikuchi, K., Sato, S., Ihn, H., Grotendorst, G.R. & Takehara, K. (1995) Significant correlation between connective tissue growth factor gene expression and skin sclerosis in tissue sections from patients with systemic sclerosis. *J. Invest. Dermatol.*, **105**, 280-284.
- Ito, Y., Aten, J., Bende, R.J., Oemar, B.S., Rabelink, T.J., Weening, J.J. & Goldschmeding, R. (1998) Expression of connective tissue growth factor in human renal fibrosis. *Kidney Int.*, **53**, 853-861.
- Jester, J.V., Petroll, W.M., Barry, P.A. & Cavanagh, H.D. (1995) Expression of alpha-smooth muscle (alpha-SM) actin during corneal stromal wound healing. *Invest. Ophthalmol. Vis. Sci.*, **36**, 809-819.
- Li, D.Q. & Tseng, S.C. (1995) Three patterns of cytokine expression potentially involved in epithelial-fibroblast interactions of human ocular surface. *J. Cell. Physiol.*, **163**, 61-79.
- Nishida, T., Nakagawa, S., Awata, T., Ohashi, Y., Watanabe, K. & Manabe, R. (1983a) Fibronectin promotes epithelial migration of cultured rabbit cornea in situ. *J. Cell Biol.*, **97**, 1653-1657.
- Nishida, T., Ohashi, Y., Awata, T. & Manabe, R. (1983b) Fibronectin. A new therapy for corneal trophic ulcer. *Arch. Ophthalmol.*, **101**, 1046-1048.
- Ohji, M., SundarRaj, N. & Thoft, R.A. (1993) Transforming growth factor-beta stimulates collagen and fibronectin synthesis by human corneal stromal fibroblasts in vitro. *Curr. Eye Res.*, **12**, 703-709.
- Pi, L., Ding, X., Jorgensen, M., Pan, J.J., Oh, S.H., Pintilie, D., Brown, A., Song, W.Y. & Petersen, B.E. (2008) Connective tissue growth factor with a novel fibronectin binding site promotes cell adhesion and migration during rat oval cell activation. *Hepatology*, **47**, 996-1004.
- Secker, G.A., Shortt, A.J., Sampson, E., Schwarz, Q.P., Schultz, G.S. & Daniels, J.T. (2008) TGFbeta stimulated re-epithelialisation is regulated by CTGF and Ras/MEK/ERK signalling. *Exp. Cell Res.*, **314**, 131-142.
- Sharma, A., Mehan, M.M., Sinha, S., Cowden, J.W. & Mohan, R.R. (2009) Trichostatin A inhibits corneal haze in vitro and in vivo. *Invest. Ophthalmol. Vis. Sci.*, **50**, 2695-2701.
- Thoft, R.A. & Friend, J. (1983) The X, Y, Z hypothesis of corneal epithelial maintenance. *Invest. Ophthalmol. Vis. Sci.*, **24**, 1442-1443.
- Watanabe, K., Nakagawa, S. & Nishida, T. (1987) Stimulatory effects of fibronectin and EGF on migration of corneal epithelial cells. *Invest. Ophthalmol. Vis. Sci.*, **28**, 205-211.
- Wilson, S.E., He, Y.G. & Lloyd, S.A. (1992) EGF, EGF receptor, basic FGF, TGF beta-1, and IL-1 alpha mRNA in human corneal epithelial cells and stromal fibroblasts. *Invest. Ophthalmol. Vis. Sci.*, **33**, 1756-1765.
- Wilson, S.E., Liu, J.J. & Mohan, R.R. (1999) Stromal-epithelial interactions in the cornea. *Prog. Retin. Eye Res.*, **18**, 293-309.
- Yoshida, K. & Munakata, H. (2007) Connective tissue growth factor binds to fibronectin through the type I repeat modules and enhances the affinity of fibronectin to fibrin. *Biochim. Biophys. Acta*, **1770**, 672-680.

Reduction in Intraocular Pressure by the Instillation of Eye Drops Containing Disulfiram Included with 2-Hydroxypropyl- β -cyclodextrin in Rabbit

Yoshimasa ITO,^{*,a,b} Noriaki NAGAI,^a and Yoshikazu SHIMOMURA^c

^a Faculty of Pharmacy, Kinki University; ^b Pharmaceutical Research and Technology Institute, Kinki University; 3-4-1 Kowakae, Higashi-Osaka, Osaka 577-8502, Japan; and ^c Department of Ophthalmology, Kinki University School of Medicine; 377-2 Ohno-Higashi, Osaka-Sayama, Osaka 589-8511, Japan.

Received May 18, 2010; accepted June 3, 2010; published online June 8, 2010

We have studied the effect of disulfiram (DSF) solution containing 2-hydroxypropyl- β -cyclodextrin and hydroxypropylmethylcellulose (DSF eye drops) on intraocular pressure (IOP) in experimentally induced ocular hypertension in rabbits. In both *in vitro* and *in vivo* transcorneal penetration experiments using rabbit corneas, only diethyldithiocarbamate (DDC) was detected in the aqueous humor, while DSF was not detected. The amount of DDC penetration for 0.25% DSF eye drops was about 4-fold that for 0.1% DSF eye drops in *in vivo* transcorneal penetration experiments. The elevation in IOP was induced by the rapid infusion of 5% glucose solution (15 ml/kg of body weight) through the marginal ear vein, and IOP was measured with an electronic tonometer. The induced elevation in IOP was reduced by the instillation of 0.1–0.5% DSF eye drops, and the IOP-reducing effect increased with the increase in DSF concentration in the drops. Nitric oxide (NO) levels increased in the aqueous humor following the infusion of the 5% glucose solution, and this increase was also suppressed by the instillation of DSF eye drops. In conclusion, the present study demonstrates that the instillation of DSF eye drops has an IOP-reducing effect in rabbits with experimentally induced ocular hypertension, probably caused by the suppression of NO production.

Key words glaucoma; nitric oxide; disulfiram; 2-hydroxypropyl- β -cyclodextrin; hydroxypropylmethylcellulose

Glaucoma is characterized by nerve degeneration that causes the disappearance of retinal ganglion cells, visual field loss and excavation of the optic disk, and ophthalmopathy.^{1,2)} It is one of the most common causes of visual impairment and blindness throughout the world and is more common in the elderly.³⁾ The major risk factor for glaucoma is elevated intraocular pressure (IOP), which leads to apoptosis and loss of retinal ganglion cells.⁴⁾ In treating glaucoma, the focus is on reducing IOP, and retinal and optic nerve damage. However, the retinal and optic nerve damage that result from elevated IOP are not satisfactorily controlled by the current therapies. Therefore, the search for successful therapies for glaucoma is a high priority.

Nitric oxide (NO) is synthesized from the guanidino-nitrogen of L-arginine and molecular oxygen by nitric oxide synthase (NOS). Endothelial NOS and neuronal NOS are present in most ocular tissues, including those responsible for aqueous dynamics, *i.e.* the ciliary processes, ciliary muscle and trabecular meshwork.^{5–7)} NO causes relaxation of the ciliary muscle and trabecular meshwork.^{8,9)} The relaxation of the ciliary muscle tends to decrease trabecular outflow facility and increase uveoscleral outflow, while relaxation of the trabecular meshwork increases trabecular outflow facility. Thus the effects of NO on IOP vary depending upon the site of action. On the other hand, recently, Kiel *et al.*¹⁰⁾ reported that the systemic inhibition of NOS by *N*^G-nitro-L-arginine methyl ester (L-NAME) causes a large, rapid decrease in IOP by due to ciliary vasoconstriction in rabbits. Therefore, agents that inhibit NOS in the blood vessel of ciliary body might prove useful in the treatment of glaucoma.

Diethyldithiocarbamate (DDC) is a potent NOS inhibitor and radical scavenger.^{11,12)} However, DDC is unstable in neutral solution, and is not able to penetrate through the cornea into the aqueous humor.¹³⁾ Disulfiram (DSF), a dimer of

DDC, has long been used to treat alcoholic syndrome without severe side effects.¹⁴⁾ However, its application in the ophthalmic field is limited due to its poor water solubility.

Cyclodextrins are cyclic oligosaccharides comprising *R*-D-glucose linked by *R*-(1–4) glucosidic bonds. Natural cyclodextrins and their synthetic derivatives have been studied extensively to improve certain properties such as their solubility, stability, and/or bioavailability.¹⁵⁾ 2-Hydroxypropyl- β -cyclodextrin (HP β CD) is a cyclic oligosaccharide with a hydrophilic outer surface and a lipophilic cavity that is capable of forming inclusion complexes with many lipophilic drugs by taking up the drug molecule, or part of it, into its lipophilic cavity.^{16,17)} In aqueous solution, hydroxypropylmethylcellulose (HPMC), a water-soluble polymer, increases the solubilizing effect of cyclodextrins on lipophilic drugs by increasing the stability constants of the drug/cyclodextrin inclusions.¹⁸⁾ We previously found that HP β CD and HPMC increase the solubility of DSF, and solve the problem of its poor water solubility.¹⁹⁾ In this study, we investigated the effect of DSF solutions containing HP β CD and HPMC (DSF eye drops) on IOP in rabbits.

MATERIALS AND METHODS

Animals Male Japanese albino rabbits, 2.5–3.0 kg, were used in this study. They were housed under standard conditions (12 h/d fluorescent light (07:00–19:00), 25 °C room temperature) and allowed free access to a commercial diet (CR-3, Clea Japan Inc., Tokyo) and water. All procedures were performed in accordance with the Kinki University Faculty of Pharmacy Committee Guidelines for the Care and Use of Laboratory Animals and the Association for Research in Vision and Ophthalmology resolution on the use of animals in research.

* To whom correspondence should be addressed. e-mail: itoyoshi@phar.kindai.ac.jp

Reagents DSF was kindly donated by Ouchi Shinko Chemical Industrial Co., Ltd. (Tokyo, Japan). HP β CD (average molar substitution, 0.6; average MW, 1380) was purchased from Nihon Shokuhin Kako Co., Ltd. (Tokyo, Japan). HPMC was provided by Shin-Etsu Chemical Co., Ltd. (Tokyo, Japan). Benzalkonium chloride was obtained from Kanto Chemical Co., Inc. (Tokyo, Japan), and 0.4% Benoxil was provided by Santen Pharmaceutical Co., Ltd. (Osaka, Japan). All other chemicals used were of the highest purity commercially available.

Preparation of Eye Drops Containing DSF Included with HP β CD HP β CD was added to saline containing 0.005% benzalkonium chloride along with DSF fine powder, and then the HPMC was added to the solution. The mixture was stirred for 24 h in the dark at room temperature and filtered through a Minisart CE (pore size of 0.20 μ m, Costar, Cambridge, MA, U.S.A.). The adsorption of DSF was not observed by filtration. The compositions of the DSF eye drops are shown in Table 1.

In Vitro Transcorneal Penetration of DDC from DSF Eye Drops The *in vitro* transcorneal penetration of DDC from DSF eye drops was examined using the method of Iwata *et al.*²⁰⁾ Adult Japanese albino rabbits weighing 2.5 to 3.0 kg were killed by injecting a lethal dose of pentobarbital into the marginal ear vein. The eyes were removed and the corneas were carefully separated from other ocular tissues. The individual corneas were placed on a methacrylate cell designed for transcorneal penetration studies. The side of the chamber (donor chamber) exposed to the exterior surface of the cornea was filled with 0.1 or 0.25% DSF eye drops. The other side of the chamber (reservoir chamber) was filled with 10 mM 4-(2-hydroxyethyl)-1-piperazine ethanesulfonic acid (HEPES) buffer (pH 7.4) containing 136.2 mM NaCl, 5.3 mM KCl, 1.0 mM K₂HPO₄, 1.7 mM CaCl₂ and 5.5 mM glucose. The experiments were performed at 35 °C for 6 h. Fifty microliters of sample solution was withdrawn from the reservoir chamber at the indicated time intervals and replaced with the same volume of buffer. DSF and DDC concentrations in the samples were determined by the following HPLC method. Fifty microliters of filtrate was added to 100 μ l methanol containing 0.25 μ g indomethacin (internal standard), and the mixture solution were filtered through a Chromatodisk 4A (pore size 0.45 μ m, Kurabo Industries Ltd., Osaka, Japan). The solution (10 μ l) was injected into a Mightysil RP-18 (3 μ m, column size: 2.0 mm \times 50 mm) column (Kanto Chemical Co., Inc., Tokyo, Japan) using a Shimadzu LC-10AD system equipped with a column oven CTO-6A (Shimadzu Corp., Kyoto, Japan). The mobile phase consisted of 45% acetonitrile containing 0.1% trifluoroacetic acid at a flow rate of 0.25 ml/min, the column temperature was 35 °C, and the wavelength for detection was 215 nm.²¹⁾ Corneal viability was monitored by measuring thickness

(0.0625 cm, average for 5 rabbits, no significant changes in thickness was observed over the 6 h period).

In Vivo Transcorneal Penetration of DDC from DSF Eye Drops The *in vivo* transcorneal penetration of DDC from DSF eye drops was determined as described by Meisner *et al.*²²⁾ Adult Japanese albino rabbits weighing 2.5 to 3.0 kg were anesthetized by injecting pentobarbital (0.6 mg/kg) through the marginal ear vein, and a topical anesthetic (0.4% Benoxil) was instilled into each eye 3 min before sampling of the aqueous humor. Then, a 29 gauge injection needle connected to silicon tubing (inner diameter: 0.5 mm, Fuji Systems Co., Tokyo, Japan) joined to a 25 μ l microsyringe (Ito Corp., Tokyo, Japan) was inserted into the eye to obtain aqueous humor samples, and 50 μ l of 0.1, 0.25 or 0.5% DSF eye drops was instilled into the eyes of the rabbits. The aqueous humor samples (5 μ l each) were removed from the anterior chamber of the eye for 0–90 min. The DSF and DDC concentrations were determined by HPLC as described above.

The DDC concentration data in the aqueous humor after a single injection of 20 μ l of DDC solution into the anterior chamber of the eye were analyzed according to Eq. 1²³⁾:

$$C_{AH} = C_0 \cdot e^{-k_e \cdot t} \quad (1)$$

where C_{AH} is the DDC concentration in the aqueous humor at time t , C_0 is the initial concentration of DDC in the aqueous humor, and k_e is the elimination rate constant of DDC from the aqueous humor. The k_e obtained in 5 experiments was 0.0502/min.

The DDC concentration data in the aqueous humor after the instillation of 50 μ l of DSF eye drops were analyzed according to Eq. 2:

$$C_{AH} = \frac{k_a \cdot F \cdot X}{V_d \cdot (k_a - k_e)} (e^{-k_e \cdot (t-\tau)} - e^{-k_a \cdot (t-\tau)}) \quad (2)$$

where C_{AH} is the DDC concentration in the aqueous humor, X is the dose of the DSF eye drop instillation, k_a is the absorption rate constant, V_d is the distribution volume (anterior chamber, *ca.* 150 μ l), F is the fraction of DDC absorption, and τ is the lag time.²³⁾ The area under the DDC concentration–time curve (AUC_{DDC}) was calculated according to the following equation (Eq. 3):

$$AUC_{DDC} = \int_0^t C_{DDC} dt \quad (3)$$

Briefly, AUC was determined according to the trapezoidal rule up to the last DDC concentration measurement point.

Measurement of Intraocular Pressure in Rabbits The experiment was carried out according to Bonomi *et al.*²⁴⁾ The IOP in rabbits was measured with an electronic tonometer (Medtronic SOLAN, Jacksonville, FL, U.S.A.) under surface anesthesia (0.4% Benoxil). IOP elevation was induced by the rapid infusion of 5% glucose solution through the rabbit marginal ear vein. The amounts injected were 15 ml/kg of body weight and the infusion was accomplished in all animals within 20 s. The various eye drops were instilled 30 min prior to the infusion of the 5% glucose solution. The area under the curve (AUC_{IOP}) of the IOP (mmHg) *versus* time (min) (the area under IOP–time curve) was calculated as the difference of AUC in rabbits with or without the infusion of 5%

Table 1. Formulations of DSF Eye Drops

	Content (%)		
	DSF	HP β CD	HPMC
0.1% DSF eye drops	0.10	1.1	0.1
0.25% DSF eye drops	0.25	3.0	0.1
0.5% DSF eye drops	0.50	5.0	0.1

glucose solution through the marginal ear vein. ΔAUC_{IOP} was calculated according to the following equation (Eq. 4):

$$\Delta AUC_{IOP} = AUC_{IOP} \text{ of saline instilled rabbit} - AUC_{IOP} \text{ of DSF eye drops instilled rabbit} \quad (4)$$

Measurement of NO Levels in the Aqueous Humor

Adult Japanese albino rabbits weighing 2.5 to 3.0 kg were anesthetized by injecting pentobarbital (0.6 mg/kg) through the marginal ear vein, and a topical anesthetic (0.4% Benoxil) was instilled into each eye 3 min before sampling of the aqueous humor. Then, a 29 gauge injection needle connected with silicon tubing (inner diameter: 0.5 mm, Fuji Systems Co., Tokyo, Japan) joined to a 25 μ l microsyringe (Ito Corp., Tokyo, Japan) was inserted into the eye to obtain aqueous humor samples, and 50 μ l of DSF eye drops was instilled into the eyes. Aqueous humor samples (5 μ l each) were collected from the anterior chamber of the eye, and the NO levels in the aqueous humor were measured using a Hitachi F-3000 Fluorescence Spectrophotometer (Hitachi, Tokyo, Japan) and NO₂/NO₃ Assay Kit-F II (Wako, Osaka, Japan) according to the manufacturer's instructions. In this paper, NO amounts reflect the levels of the NO₂⁻ and NO₃⁻ metabolites, which are the products of NO.

Statistical Analysis All values are presented as mean \pm standard error of the mean (S.E.). Unpaired Student's or Aspin-Welch's *t*-tests were used to evaluate statistical differences, and multiple groups were evaluated by one-way analysis of variance followed by Dunnett's multiple comparison. *p* values less than 0.05 were considered significant.

RESULTS

Transcorneal Penetration of DDC from DSF Eye Drops

Figure 1 shows *in vitro* transcorneal penetration of DDC from DSF eye drops using rabbit corneas. In this study, only DDC, not DSF, was detected. The amount of penetrated DDC increased after instillation of 0.1 or 0.25% DSF eye drops. There were no significant differences in the amount of penetration between the two DSF eye drop formulations. Figure 2 shows the DDC concentrations in the aqueous humor after the instillation of 0.1 or 0.25% DSF eye drops into rabbit eyes, and Table 2 summarizes the pharmacokinetic pa-

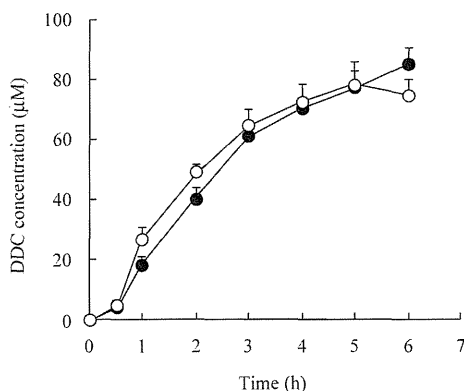


Fig. 1. *In Vitro* Transcorneal Penetration of DDC from DSF Eye Drops
The donor chamber with the exterior surface of the cornea was filled with 0.1 or 0.25% DSF eye drops. 0.1% DSF eye drops (○), 0.25% DSF eye drops (●). The data represent the means \pm S.E. of 5 rabbit corneas.

rameters calculated from the *in vivo* transcorneal penetration data. In the aqueous humor, only DDC was detected, with a peak concentration observed at 20 min after the instillation of 0.25% DSF eye drops. In contrast to the *in vitro* transcorneal penetration results, the amount of DDC penetration for the 0.25% DSF eye drops was higher than that for the 0.1% eye drops, and the values of AUC_{DDC} and k_a for the 0.25% DSF eye drops were approximately 2.5-fold higher in comparison with those of the 0.1% DSF eye drops.

Effect of DSF Eye Drops on IOP in Rabbit Figure 3 shows the effects of the instillation of DSF eye drops on IOP in rabbits with experimentally induced ocular hypertension,

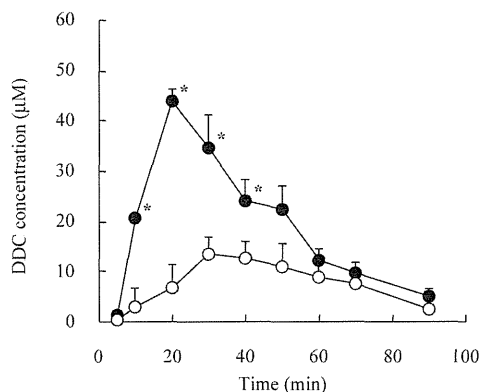


Fig. 2. *In Vivo* Transcorneal Penetration of DDC from DSF Eye Drops
Rabbits were instilled with 50 μ l of 0.1 or 0.25% DSF eye drops. 0.1% DSF eye drop instilled rabbits (○), 0.25% DSF eye drop instilled rabbits (●). The data represent the means \pm S.E. of 5 rabbit corneas. **p* < 0.05, vs. 0.1% DSF eye drops instilled rabbit.

Table 2. Pharmacokinetic Parameters for the *in Vivo* Transcorneal Penetration of DDC Released from DSF Eye Drops

	AUC_{DDC} ($\mu\text{M} \cdot \text{min}$)	k_a (min)	τ (min)
0.1% DSF eye drops	738 \pm 62	0.025 \pm 0.004	5.84 \pm 0.67
0.25% DSF eye drops	1835 \pm 313*	0.072 \pm 0.007*	4.99 \pm 0.22

AUC_{DDC} , the area under the DDC concentration-time curve; k_a , absorption rate constant; τ , lag time. The data are presented as means \pm S.E. of 5 independent rabbits. **p* < 0.05, vs. 0.1% DSF eye drops.

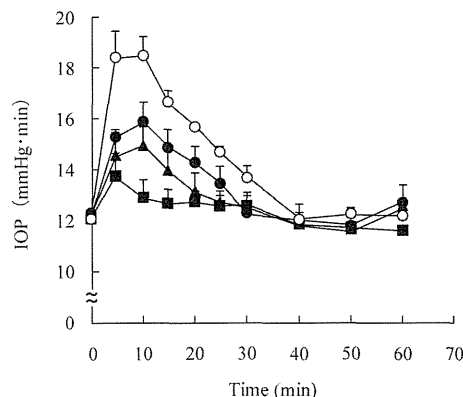


Fig. 3. Effect of DSF Eye Drops on IOP in Rabbits Receiving a Rapid Infusion of 5% Glucose Solution
Rabbits receiving a rapid infusion of 5% glucose solution were instilled with 50 μ l of saline or DSF eye drops. Saline instilled rabbits (○), 0.1% DSF eye drop instilled rabbits (●), 0.25% DSF eye drop instilled rabbits (▲), 0.5% DSF eye drop instilled rabbits (■). The data represent as means \pm S.E. of 5 independent rabbits.

Table 3. The IOP-Reducing Effect of DSF Eye Drops in Rabbits Receiving Rapid Infusions with 5% Glucose Solution

	ΔAUC_{IOP} (mmHg·min)
0.1% DSF eye drops	52.4±4.9
0.25% DSF eye drops	61.8±5.4
0.5% DSF eye drops	107.8±14.7*

ΔAUC_{IOP} was calculated as the difference of AUC_{IOP} of saline instilled rabbit and AUC_{IOP} of DSF eye drops instilled rabbit. The data represent the means±S.E. of 5 independent rabbits. * $p<0.05$, vs. 0.1% DSF eye drops.

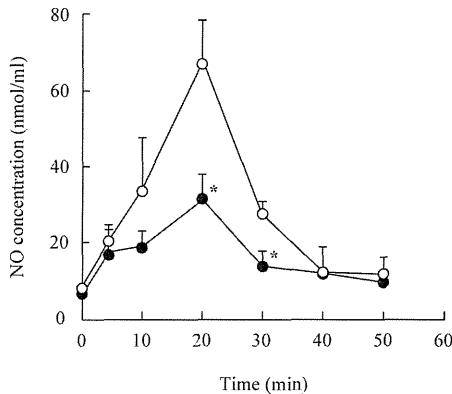


Fig. 4. Effect of DSF Eye Drops on NO in Rabbit Rapid Infused with 5% Glucose Solution

The rabbits rapid infused with 5% glucose solution were instilled with 50 μ l of saline or 0.5% DSF eye drops. Saline instilled rabbit (\circ), 0.5% DSF eye drops instilled rabbit (\bullet). The data are represent the means±S.E. of 5 independent rabbits. * $p<0.05$, vs. saline instilled rabbit.

and Table 3 shows the IOP-reducing effect of DSF eye drops. The elevation of IOP in rabbits was induced by the rapid infusion of 5% glucose solution (15 ml/kg) through the marginal ear vein. The IOP was highest 10 min after the infusion, and returned to the pre-infusion level by 50 min after the infusion. Rabbits instilled with DSF eye drops showed a significantly reduced level of IOP elevation compared with rabbits instilled with saline, and the IOP-reducing effect increased with the increase in the DSF concentration of the eye drops (Table 3). Figure 4 shows the changes of NO levels in the aqueous humor of rabbits instilled with saline or 0.5% DSF eye drops. NO levels in the aqueous humor of rabbits rose following the rapid infusion of 5% glucose solution into the marginal ear vein, and reached a maximum at 20 min. The instillation of DSF eye drops also reduced the degree of NO elevation in the aqueous humor.

DISCUSSION

Glaucoma is a major cause of blindness, with an estimated 70 million people affected worldwide. Over the course of their lives, 10% of these patients will become bilaterally blind.³⁾ However, for reasons of effectiveness and safety, a potent anti-glaucoma drug for human use has not yet been introduced. From the view point of the recent steep increase in the number of patients with glaucoma in modern aging societies, the development of effective and safe anti-glaucoma drugs is highly anticipated. In this study, we investigated the effects of DSF eye drops on IOP.

The safety of eye drops is an important factor. It has been reported that HP β CD ranks second in safety to γ -CD in a va-

riety of CD derivatives used for eye drop applications.²⁵⁾ Moreover, Jansen *et al.*²⁶⁾ reported no irritation to eye membranes by HP β CD solutions less than 12.5%. Therefore, we used 1—5% HP β CD, which is low in comparison with the concentrations used in that report, and decided the DSF concentrations to be used in eye drops.¹⁹⁾

In both *in vitro* and *in vivo* transcorneal penetration experiments using rabbit corneas only DDC was detected in the reservoir side or aqueous humor. We previously reported a sulfhydryl-rich protein, aldehyde dehydrogenase 3A1 (ALDH3A1), which is related to the conversion of DSF to DDC, and exists in abundance in the corneal stroma and endothelium.^{19,27,28)} Therefore, DSF in HP β CD solutions containing HPMC may be converted to DDC *via* catalysis by ALDH3A1 in the cornea. The amount of DDC penetration showed no significant difference between 0.1 and 0.25% DSF eye drops in the *in vitro* transcorneal penetration experiments (Fig. 1). In contrast, in the *in vivo* transcorneal penetration experiments, the amount of DDC penetration was about 4-fold higher in the case of the 0.25% DSF eye drops than the 0.1% DSF eye drops, and the values of AUC_{DDC} and k_a were also higher for the 0.25% DSF eye drops than the 0.1% DSF eye drops (Fig. 2). In the *in vitro* transcorneal penetration experiments, the viscosity and corneal contact area of the 0.1 and 0.25% DSF eye drops were almost the same, since the DSF eye drops were completely stirred in the chamber. These results suggest that the absorption rate for transcorneal DDC penetration is regulated by the viscosity and corneal contact area of the DSF eye drops. Therefore, we measured the viscosity the two DSF drop preparations. The viscosity of the 0.25% DSF eye drops was higher than that of the 0.1% DSF eye drops (1.85 mm²/s for the 0.1% DSF eye drops, 2.01 mm²/s for the 0.25% DSF eye drops; measured at 25 °C by an Uberode type viscometer). It was known when the eye drops was lost from tear film within 30 s—2 min, while a small amount remained associated with conjunctival tissue. On the other hand, the increase in viscosity of the eye drops remained a higher storage on the surface of a cornea.²⁹⁾ These suggest that the 0.25% DSF eye drops have a higher storage on the surface of a cornea, and this lead to the higher absorption rate for 0.25% DSF eye drops than the 0.1% DSF eye drops. In addition, free DSF and HP β CD-included DSF coexists both in 0.1 and 0.25% DSF solutions. Moreover, the concentrations of free DSF in those solutions are almost same. Therefore, the free DSF related strongly to the transcorneal penetration.

The intravenous administration of a 5% glucose solution is a simple and reproducible technique for the screening of anti-glaucoma agents.²⁴⁾ In this study, the IOP in rabbits receiving a rapid infusion of 5% glucose solution initially rose, and returned to baseline levels by 50 min after infusion. This indicates that the IOP elevation in this experiment may provide a suitable model for acute glaucoma. The degree of IOP elevation in rabbits receiving a rapid infusion of 5% glucose solution was reduced by the instillation of DSF eye drops with both 0.1 and 0.25% DSF eye drops providing IOP-reducing effects sufficient to protect against glaucoma. In addition, the IOP-reducing effect was greater for the higher DSF concentration (Table 3). These results demonstrate that DSF eye drops containing 0.1 or 0.25% may be useful agents for the treatment of glaucoma.

It is important to clarify the mechanism by which DSF eye drops protect against the elevation in IOP. Shah *et al.*³⁰⁾ reported that the rapid infusion of a 5% glucose solution into rabbits leads to a reduction in blood osmolarity, which leads to the transfer of water into the eye thus causing the elevation in IOP. Kiel *et al.*^{10,31)} reported that the inhibition of NOS by L-NAME causes a decrease in water production by due to ciliary vasoconstriction in rabbits, resulting in a decrease in IOP. In addition, it was known that the IOP elevation in rabbits receiving a rapid infusion of 5% glucose solution used this study was caused by rapidly aqueous humor production.²⁴⁾ In our previous study, we reported that DSF eye drops prevent excess NO production in the eye.³²⁾ We used 0.5% DSF eye drops to clarify the IOP-reducing mechanism of DSF eye drops, because the higher concentration makes it easier to clarify the IOP-reducing effects. NO levels in the aqueous humor of rabbits receiving the rapid infusion of 5% glucose solution increased, and the instillation of 0.5% DSF eye drops reduced this increase (Fig. 4). The instillation of DSF eye drops did not affect the IOP of normal rabbit (without the rapid infusion of 5% glucose solution, data not shown). Taking these findings together, we hypothesize that the DSF eye drops penetrate the cornea, and that DSF is converted in the cornea to DDC by ALDH3A1. This DDC may cause a reduction in water production by inhibiting NO production, resulting in a reduction in IOP. On the other hand, the elevation of IOP occurs prior to the induction of NO in the aqueous humor. In this study, the NO amounts reflect the levels of the NO₂⁻ and NO₃⁻ metabolites, which are the products of NO. Therefore, the high NO levels by 20 min after the infusion may show metabolites of NO. As incipient NO produced in the eye may be consumed for the ciliary vasoconstriction, the apparent enhancement of NO in the aqueous humor may not change.

Further studies are needed to elucidate the precise mechanisms of the IOP-reducing effect of DSF eye drops. Therefore, we are now investigating the effect of DSF eye drops on aqueous production.

In conclusion, the present study demonstrates that IOP and NO levels increase in rabbits receiving a rapid infusion of 5% glucose solution, and the instillation of DSF eye drops reduces these increases. The instillation of DSF eye drops has a potent IOP-reducing effect in rabbits with experimentally induced high IOP, probably by inhibiting the elevation in NO levels. These findings provide significant information that can be used in designing further studies to develop anti-glaucoma drugs.

REFERENCES

1) Armaly M. F., Krueger D. E., Maunder L., Becker B., Hetherington J.

- Jr., Kolker A. E., Levene R. Z., Maumenee A. E., Pollack I. P., Shaffer R. N., *Arch. Ophthalmol.*, **98**, 2163—2171 (1980).
- 2) Quigley H. A., Addicks E. M., Green W. R., Maumenee A. E., *Arch. Ophthalmol.*, **99**, 635—649 (1981).
- 3) Quigley H. A., *Br. J. Ophthalmol.*, **80**, 389—393 (1996).
- 4) Guo L., Moss S. E., Alexander R. A., Ali R. R., Fitzke F. W., Cordeiro M. F., *Invest. Ophthalmol. Vis. Sci.*, **46**, 175—182 (2005).
- 5) Osborne N. N., Barnett N. L., Herrera A. J., *Brain Res.*, **610**, 194—198 (1993).
- 6) Nathanson J. A., McKee M., *Ophthalmol. Vis. Sci.*, **36**, 1765—1773 (1995).
- 7) Meyer P., Champion C., Schlotzer S. U., Flammer J., Haefliger I. O., *Curr. Eye Res.*, **18**, 375—380 (1999).
- 8) Wiederholt M., Sturm A., Lepple W. A., *Invest. Ophthalmol. Vis. Sci.*, **35**, 2515—2520 (1994).
- 9) Goh Y., Hotehama Y., Mishima H. K., *Invest. Ophthalmol. Vis. Sci.*, **36**, 1188—1192 (1995).
- 10) Kiel J. W., Reitsamer H. A., Walker J. S., Kiel F. W., *Exp. Eye Res.*, **73**, 355—364 (2001).
- 11) Mulsch A., Schray-Utz B., Mordvintcev P. I., Hauschildt S., Busse R., *FEBS Lett.*, **321**, 215—218 (1993).
- 12) Schreck R., Meier B., Mannel D. N., Droge W., Baeuerle P. A., *J. Exp. Med.*, **175**, 1181—1194 (1992).
- 13) Ito Y., Cai H., Koizumi Y., Hori R., Terao M., Kimura T., Takagi S., Tomohiro M., *Biol. Pharm. Bull.*, **23**, 327—333 (2000).
- 14) Rall T. W., "The Pharmacological Basis of Therapeutics," 8th ed., ed. by Gilman A. G., Rall T. W., Nies A. S., Taylor P., Perfarmon Press, New York, 1990, pp. 378—379.
- 15) Irie T., Uekama K., *J. Pharm. Sci.*, **86**, 147—162 (1997).
- 16) Mueller B. W., Brauns U., *Int. J. Pharm.*, **26**, 77—88 (1985).
- 17) Kristinsson J. K., Fridriksdottir H., Thorisdottir S., Sigurdardottir A. M., Stefansson E., Loftsson T., *Invest. Ophthalmol. Vis. Sci.*, **37**, 1199—1203 (1996).
- 18) Wang S., Li D., Ito Y., Liu X., Zhang J., Wu C., *J. Pharm. Pharmacol.*, **56**, 1251—1257 (2004).
- 19) Nagai N., Takeda M., Ito Y., Takeuchi T., Kamei A., *Biol. Pharm. Bull.*, **30**, 1529—1534 (2007).
- 20) Iwata S., Osada Y., Ogino H., *Yakugaku Zasshi*, **100**, 402—406 (1980).
- 21) Ito Y., Cai H., Koizumi Y., Nakao M., Terao M., *Curr. Eye Res.*, **18**, 292—299 (1999).
- 22) Meisner D., Pringle J., Mezei M., *Int. J. Pharm.*, **55**, 105—113 (1989).
- 23) Yamaoka K., Tanigawara Y., Nakagawa T., Uno T., *J. Pharmacobio-Dyn.*, **4**, 879—885 (1981).
- 24) Bonomi L., Tomazzoli L., Jaria D., *Invest. Ophthalmol.*, **15**, 781—784 (1976).
- 25) Saarinen S. P., Jarvinen T., Araki S. K., Watanabe H., Urtti A., *Pharm. Res.*, **15**, 1275—1280 (1998).
- 26) Jansen T., Xhonneux B., Mesens J., Borgers M., *Lens Eye Toxic. Res.*, **7**, 459—468 (1990).
- 27) King G., Holmes R., *J. Exp. Zool.*, **282**, 12—17 (1998).
- 28) Nagai N., Inomata M., Ito Y., *Biol. Pharm. Bull.*, **31**, 444—448 (2008).
- 29) Schultz G. S., Davis J. B., Eiferman R. A., *Cornea*, **7**, 96—101 (1988).
- 30) Shah G. B., Sharma S., Mehta A. A., Goyal R. K., *J. Cardiovasc. Pharmacol.*, **36**, 169—175 (2000).
- 31) Kiel J. W., *Exp. Eye Res.*, **69**, 413—429 (1999).
- 32) Nagai N., Ito Y., Takeuchi N., *Biol. Pharm. Bull.*, **31**, 981—985 (2008).

REVIEW

Suppression of Herpes Simplex Virus 1 Reactivation in a Mouse Eye Model by Cyclooxygenase Inhibitor, Heat Shock Protein Inhibitor, and Adenosine Monophosphate

Yoshikazu Shimomura, Shiro Higaki, and Keizo Watanabe

Kinki University School of Medicine, Osaka, Japan

Jpn J Ophthalmol 2010;54:187-190 © Japanese Ophthalmological Society 2010

Keywords: AMP, COX inhibitor, HSP Inhibitor, HSV-1 latency, HSV-1 reactivation

Introduction

It is accepted that herpes simplex virus type 1 (HSV-1) latency occurs in the trigeminal ganglion. However, our group^{1,2} and several other groups have demonstrated latent virus presence in the cornea. Negative homogenate and positive coculture provide proof of latent infection. Conventional coculture tests demonstrated HSV-1 latency in ten of the 20 eyes (50%) with herpetic stromal keratitis in the quiescent phase we examined.¹ In addition, although conventional coculture detected 50% presence, polymerase chain reaction (PCR) demonstrated HSV-1 latency in the corneas of 80% of these cases.¹

Various methods have been tried to suppress HSV-1 reactivation. Studies have shown that acyclovir,³ propranolol,⁴ thymidine kinase inhibitor,⁵ helicase-primase inhibitor,⁶ bupropion,⁷ and oral cyclooxygenase (COX) inhibitor^{8,9} effectively lower HSV-1 recurrence rates. However, the improvements registered did not prove sufficient.

Suppressing HSV-1 Reactivation

In our current study,^{10,11} seven medications were investigated for their efficacy in suppressing HSV-1 reactivation. These medications were oral etodolac, bromfenac sodium

(Na) eye drops, pranoprofen eye drops, oral ascorbic acid,¹² oral zinc,¹³ intramuscular adenosine monophosphate (AMP),¹⁴ and intraperitoneal geldanamycin.¹⁵ Etodolac, bromfenac Na eye drops, and pranoprofen are COX inhibitors. Oral etodolac is dominant in COX-2 inhibition, bromfenac Na eye drops, too, are dominant in COX-2 inhibition,¹⁶ whereas pranoprofen eye drops are not COX-2-specific.¹⁷ Ascorbic acid is vitamin C, and geldanamycin is a heat shock protein inhibitor.

Methods

Mice corneas were inoculated with 2.5×10^4 plaque forming units (PFU) of HSV-1 strain McKrae. Four weeks later, mice confirmed to have latent HSV-1 were treated with one of the following: oral etodolac (Hypen, Nihonshinyaku, Tokyo, Japan), bromfenac Na eye drops (Bronuck, Senjyu, Tokyo, Japan), pranoprofen eye drops (Proranon, Santen, Tokyo, Japan), oral ascorbic acid (Sigma, St Louis, MO, USA), oral zinc (Sigma), intramuscular AMP (Nacalai Tesque, Kyoto, Japan), and intraperitoneal geldanamycin (InvivoGen, San Diego, CA, USA) for 4 days. As controls, saline solution eye drops (saline solution injection, Otsuka Pharmaceutical, Tokushima, Japan), oral saline solution, intramuscular saline solution, and intraperitoneal dimethyl sulfoxide (DMSO, Wako, Osaka, Japan) were used. These treatments continued from postinfection (PI) day 31 to 34 (PI day 25 to 29 in the ascorbic acid, zinc, AMP, and geldanamycin groups). The mice were given an intravenous injection of cyclophosphamide on PI day 32 (PI day 28 in the ascorbic acid, zinc, AMP, and geldanamycin groups).

Received: September 11, 2009 / Accepted: February 24, 2010

Correspondence and reprint requests to: Yoshikazu Shimomura, Kinki University School of Medicine, 377-2 Ono-Higashi, Osaka Sayama, Osaka 589-8511, Japan
e-mail: yoshis@med.kindai.ac.jp

and another intravenous injection of dexamethasone on PI day 33 (PI day 29 in the ascorbic acid, zinc, AMP, and geldanamycin groups). Seven hours after the dexamethasone injections, the mice were heated for 10 min in a hot water bath at 43°C. At 24 h after the hyperthermia, the mouse ocular surfaces were swabbed for the culture of the infectious virus and the mice were killed. Plaque assay and real-time PCR were performed on the eye balls and trigeminal ganglia.

Results

Table 1 shows the eye swab results for the etodolac, bromfenac Na, and pranoprofen groups.¹⁰ When the stimulation for reactivation was performed, ten of 24 eyes (41.7%) of the bromfenac Na group, five of ten eyes (50.0%) of the etodolac group, and 17 of 25 eyes (68%) of the pranoprofen group showed positive results. However, compared with the results for the saline solution group (16 of 22 eyes, 72.7%), only the bromfenac Na group was significantly different ($P = 0.033$, Fisher's exact probability test). On the other hand, all groups had a positivity rate of 0% in eye swab results when no stimulation was performed.

HSV DNA copy numbers in both the eyes and trigeminal ganglia were also assessed (Table 2).¹⁰ Although none of the three drug-treated groups showed any significant differences from the saline solution group ($P > 0.05$, Welch's t test), the average copy number of viral DNA in the trigemi-

nal ganglia of the mice treated with either etodolac or bromfenac Na eye drops was about one-tenth that of the mice treated with saline solution. However, the pranoprofen eye drops demonstrated an outcome inferior by an order of magnitude to that of the bromfenac Na eye drops in TGs. We attributed this to the difference in the selectivity of the COX inhibitory effect. The HSV DNA copy numbers in the eyeballs also showed no significant difference between the saline solution and the other three, drug-treated groups. Thus, without stimulation, the three drug-treated groups showed no significant differences from the saline solution group in the viral DNA copy number in either the eyes or the TGs.

Table 3 shows plaque assay results of the oral ascorbic acid, oral zinc, intraperitoneal geldanamycin, and intramuscular groups.¹¹ Oral saline solution, intraperitoneal DMSO, and intramuscular saline solution were control groups. When the stimulation for reactivation was performed, only three of 22 eyes (14%) showed positive results in the intraperitoneal geldanamycin group. The geldanamycin group differed significantly from the DMSO group ($P < 0.05$, Fisher's exact probability test).

Table 4 shows the HSV DNA copy numbers in the trigeminal ganglion and the eye with reactivation.¹¹ The HSV DNA copy numbers in the trigeminal ganglia of intramuscular AMP groups showed significant differences from those of the intramuscular saline solution group ($P < 0.05$, Mann-Whitney U test). The HSV DNA copy numbers in the eyeballs showed no significant difference among the groups.

Table 1. Eye swab results¹⁰

	Saline (eye drops)	Bromfenac Na (eye drops)	Etodolac (oral)	Pranoprofen (eye drops)
With reactivation	16/22	10/24*	5/10	17/25
No. of positive eyes/total no. of eyes (%)	(72.7)	(41.7)	(50.0)	(68.0)
Without reactivation	0/6	0/6	0/6	0/4
No. of positive eyes/total no. of eyes (%)	(0)	(0)	(0)	(0)

*Significantly different from the saline group ($P = 0.033$, Fisher's exact probability test).

Table 2. The HSV DNA copy numbers in the TG and the eye with and without reactivation¹⁰

		Saline (eye drops)	Bromfenac Na (eye drops)	Etodolac (oral)	Pranoprofen (eye drops)
TG	With reactivation	9.86 ± 21.11 ×10 ² (n = 21)	6.05 ± 11.65 ×10 ¹ (n = 20)	9.38 ± 23.05 ×10 ¹ (n = 9)	5.48 ± 8.94 ×10 ² (n = 20)
	Without reactivation	5.31 ± 2.88 ×10 ¹ (n = 3)	2.37 ± 4.08 ×10 ¹ (n = 3)	3.85 ± 3.69 ×10 ¹ (n = 3)	2.95 ± 3.26 ×10 ¹ (n = 3)
Eye	With reactivation	3.73 ± 12.88 ×10 ⁻¹ (n = 21)	2.74 ± 15.21 ×10 ⁻¹ (n = 20)	8.86 ± 29.73 ×10 ⁻² (n = 12)	1.53 ± 4.32 ×10 ⁻¹ (n = 20)
	Without reactivation	2.62 ± 2.43 ×10 ⁰ (n = 5)	2.78 ± 5.43 ×10 ⁰ (n = 5)	2.88 ± 5.75 ×10 ⁰ (n = 4)	2.60 ± 5.82 ×10 ⁻¹ (n = 5)

Values are the average copy number ± SD per 100 ng of tissue DNA. HSV, herpes simplex virus; TG, trigeminal ganglion.

Table 3. Plaque assay results¹¹

		Saline (oral)	Ascorbic acid (oral)	Zinc (oral)	DMSO (intraperitoneal)	Geldanamycin (intraperitoneal)	Saline (intramuscular)	AMP (intramuscular)
TG	With reactivation	5/20 (20%)	2/15 (13%)	8/25 (32%)	11/24 (46%)	* 3/22 (14%)	5/21 (24%)	4/20 (20%)
Eye	With reactivation	6/20 (30%)	1/15 (7%)	3/26 (12%)	5/24 (21%)	4/24 (17%)	5/22 (23%)	4/22 (18%)

Values are given as the number (percentage) of HSV-1-positive samples.

AMP, adenosine monophosphate; DMSO, dimethyl sulfoxide.

*Significant difference from the DMSO group ($P < 0.05$, Fisher's exact probability test).

Table 4. HSV DNA copy numbers in the TG and the eye with reactivation¹¹

		Saline (oral)	Ascorbic acid (oral)	Zinc (oral)	DMSO (intraperitoneal)	Geldanamycin (intraperitoneal)	Saline (intramuscular)	AMP (intramuscular)
TG	With reactivation	2.72 ± 3.99 ×10 ³ (n = 20)	3.58 ± 5.47 ×10 ³ (n = 15)	1.45 ± 2.55 ×10 ³ (n = 25)	1.34 ± 3.17 ×10 ³ (n = 24)	4.89 ± 10.3 ×10 ² (n = 22)	2.30 ± 3.16 ×10 ³ (n = 21)	8.39 ± 27.2* ×10 ² (n = 20)
Eye	With reactivation	5.50 ± 14.6 ×10 ¹ (n = 20)	1.21 ± 2.02 ×10 ² (n = 15)	4.58 ± 10.1 ×10 ¹ (n = 26)	9.17 ± 24.8 ×10 ⁻¹ (n = 24)	1.08 ± 3.34 ×10 ¹ (n = 24)	2.55 ± 4.45 ×10 ¹ (n = 22)	4.50 ± 17.4 ×10 ⁻¹ (n = 22)

Values are given as average copy number ± SD per 100 ng of tissue DNA.

*Significantly different from the saline group ($P < 0.05$, Mann-Whitney U test).

Discussion

Eye swabs and real-time PCR yielded different results. Because eye swabs detect live viruses and real-time PCR can detect both live viruses and fragments of viral DNA, both methods show similar results in cases of acute infection and different results in cases of either latent infection or reactivation. We believe that in studies focusing on reactivation such as the present one, the eye swab results may be more valid than the real-time PCR results.

Bromfenac Na eye drops may have exerted their inhibitory effect on the TGs via the first trigeminal nerve branch as well as through systemic absorption. Waterbury et al.¹⁶ reported a significant effect of bromfenac eye drops on the contralateral eye and suggested the possible systemic absorption of this drug. More studies on COX gene expression in the trigeminal ganglia using semiquantitative reverse transcriptase (RT)-PCR, real-time RT-PCR, or microarray analysis would help further elucidate the mechanism by which a COX inhibitor prevents HSV reactivation.

HSV reactivation in not only a mouse model but also a rabbit and possibly also a monkey model should also be studied. Furthermore, studies on whether a combined remedy with a conventional antiviral drug such as acyclovir and a COX inhibitor or heat shock protein inhibitor would additively or synergistically enhance the inhibition of viral reactivation are also of future interest.⁹ Besides suppression of viral reactivation, another study¹⁸ concluded that a COX-2 inhibitor can effectively treat herpetic stromal keratitis. We plan to further investigate the possible efficacy of the medications tested here on herpetic stromal keratitis.

In conclusion, we showed that bromfenac Na eye drops, intramuscular AMP, and intraperitoneal geldanamycin significantly suppressed HSV-1 reactivation in our mouse model.

References

- Shimomura Y. Reactivation and latency of herpesvirus in the eye. *Ophthalmologica* 2001;215 suppl 2:15E24.
- Shimomura Y, Deai T, Fukuda M, Higaki S, Hooper LC, Hayashi K. Corneal buttons obtained from patients with HSK harbor high copy numbers of the HSV genome. *Cornea* 2007;26:190E93.
- Herpetic Eye Disease Study Group. Acyclovir for the prevention of recurrent HSV eye disease. *N Engl J Med* 1998;339:300E306.
- Kaufman HE, Varnell ED, Gebhardt BM, Thompson HW, Hill JM. Propranolol suppression of ocular HSV-1 recurrence and associated corneal lesions following spontaneous reactivation in the rabbit. *Curr Eye Res* 1996;15:680E684.
- Gebhardt BM, Wright GE, Xu H, Focher F, Spadari S, Kaufman HE. 9-(4-Hydroxybutyl)-N2-phenylguanidine (HBPG), a thymidine kinase inhibitor, suppresses herpes virus reactivation in mice. *Antiviral Res* 1996;30:87E94.
- Kaufman HE, Varnell ED, Gebhardt BM, et al. Efficacy of a helicase-primase inhibitor in animal models of ocular herpes simplex virus type 1 infection. *J Ocul Pharmacol Ther* 2008;24:34E42.
- Myles ME, Azcuy AM, Nguyen NT, et al. Bupropion (Zyban, Wellbutrin) inhibits nicotine-induced viral reactivation in herpes simplex virus type 1 latent rabbits. *J Pharmacol Exp Ther* 2004; 311:640E644.
- Kurane I, Tsuchiya Y, Sekizawa T, Kumagai K. Inhibition by indomethacin of in vitro reactivation of latent herpes simplex virus type 1 in murine trigeminal ganglia. *J Gen Virol* 1984;65:1665E1674.
- Gebhardt BM, Varnell ED, Kaufman HE. Inhibition of cyclooxygenase 2 synthesis suppresses herpes simplex virus type 1 reactivation. *J Ocul Pharmacol Ther* 2005;21:114E120.
- Higaki S, Watanabe K, Itahashi M, Shimomura Y. Cyclooxygenase (COX)-inhibiting drug reduces HSV-1 reactivation in the mouse eye model. *Curr Eye Res* 2009;34:171E176.

11. Watanabe K. New therapy to reduce HSV-1 reactivation in mouse model. *Kinki Univ Med J* 2009;34:3-9.
12. Furuya A, Uozaki M, Yamasaki H, Arakawa T, Arita M, Koyama AH. Antiviral effects of ascorbic and dehydroascorbic acids in vitro. *Int J Mol Med* 2008;22:541-545.
13. Femiano F, Gombos F, Scully C. Recurrent herpes labialis: a pilot study of the efficacy of zinc therapy. *J Oral Pathol Med* 2005;34:423-425.
14. Millhouse S, Kenny JJ, Quinn PG, Lee V, Wigdahl B. ATF/CREB elements in the herpes simplex virus type 1 latency-associated transcript promoter interact with members of the ATF/CREB and AP-1 transcription factor families. *J Biomed Sci* 1998;5:451-464.
15. Necklers LM. Can the heat shock protein 90 inhibitor geldanamycin be designed to specifically inhibit HER-2 tyrosine kinase? *Drug Resist Updat* 2000;3:203-205.
16. Waterbury LD, Silliman D, Jolas T. Comparison of cyclooxygenase inhibitory activity and ocular anti-inflammatory effects of ketorolac tromethamine and bromfenac sodium. *Curr Med Res Opin* 2006;22:1133-1140.
17. Sano M. Nonsteroidal anti-inflammatory drugs. *Iyaku J* 2003;39:83-97.
18. Banerjee K, Biswas PS, Rouse BT. Role of Stat4-mediated signal transduction events in the generation of aggressor CD4+ T cells in herpetic stromal keratitis pathogenesis. *J Interferon Cytokine Res* 2007;27:65-75.

Detection and Quantification of Pathogenic Bacteria and Fungi Using Real-Time Polymerase Chain Reaction by Cycling Probe in Patients With Corneal Ulcer

Motoki Itahashi, MD, PhD; Shiro Higaki, MD, PhD; Masahiko Fukuda, MD, PhD; Yoshikazu Shimomura, MD, PhD

Objective: To detect and quantitate the causative pathogens in patients with corneal ulcer using real-time polymerase chain reaction (PCR) by cycling probe.

Design: Clinical and laboratory study of 40 eyes of 40 patients diagnosed with corneal ulcer. Two methods were used for pathogen detection: bacterial culture and real-time PCR with the patient's corneal scrapings. Probes and primers of real-time PCR were designed to be pathogen specific for simultaneous detection of *Staphylococcus aureus*, *Staphylococcus pneumoniae*, *Pseudomonas aeruginosa*, methicillin-resistant *S aureus*, *Candida* species, and *Fusarium* species. Results by both methods were evaluated and compared.

Results: Of 40 eyes, 20 eyes had the same pathogens detected by both methods and those were *S aureus* (3 eyes; mean [SE], $3.8 [1.3] \times 10^1$ copies/sample), *S pneumoniae*

(5 eyes; mean [SE], $5.6 [5.1] \times 10^3$ copies/sample), *P aeruginosa* (8 eyes; $5.1 [4.0] \times 10^3$ copies/sample), methicillin-resistant *S aureus* (1 eye; 1.0×10^2 copies/sample), and *Candida* species (3 eyes; mean [SE], $8.8 [4.9] \times 10^3$ copies/sample). Six eyes showed negative results by both methods. Results of both methods disagreed in 14 eyes; specifically, 11 had positive PCR results only, 2 had positive culture results only, and 1 eye had positive results for different pathogens.

Conclusions: The real-time PCR assay can simultaneously detect and quantitate bacterial and fungal pathogens in patients with corneal ulcer. Real-time PCR can be a fast diagnostic tool and may be useful as an adjunct to identify potential pathogens.

Arch Ophthalmol. 2010;128(5):535-540

CORNEAL ULCER, INCLUDING bacterial keratitis, fungal keratitis, and *Acanthamoeba* keratitis, can cause corneal opacity, deteriorated visual acuity, or even lead to some lifelong complications. Bacterial culture and smear examination using corneal scrapings is the conventional method to detect causative pathogens of corneal ulcer. However, bacterial culture is time-consuming and results of smear examination depend on the laboratory technician's skill. Therefore, a fast and accurate diagnostic method is highly desirable.

In recent years, polymerase chain reaction (PCR) has been widely used for clinical bacterium¹⁻⁶ and virus-specific⁷⁻¹⁰ detection and various technologies¹¹⁻¹⁸ have been developed for the PCR assay. Multiplex PCR¹¹ with multiple primers and real-time PCR with linear probe,¹² structured probe,¹³ or cycling probe¹⁴⁻¹⁸ (Cycleave PCR; Takara Bio Inc, Shiga, Japan) are such examples.

Cycleave PCR uses a chimeric DNA-RNA-DNA probe with a strand length of

10 to 14 bases (**Figure**).¹⁴⁻¹⁸ When the probe hybridizes to its complementary target DNA, RNase H cleaves the probe at the RNA linkage and this allows emission of strong fluorescence. By measuring the intensity of the emitted fluorescence, the amount of the amplified product can be measured (Figure). As compared with linear probe or structured probe with longer-length probes, Cycleave PCR is highly specific with its cycling probe.¹⁴⁻¹⁸

In addition to real-time PCR, DNA sequencer is another method to detect causative pathogens.^{19,20} However, this method is time-consuming and complicated and thus less efficient than real-time PCR.

Despite its increasing popularity, PCR has many limitations and it is still quite a challenge to accurately identify the causative pathogens of corneal ulcers by PCR.^{5,6} Though real-time PCR¹²⁻¹⁸ is not generally available to most ophthalmologists, this technique can be useful in identifying the causative pathogens. The utility of DNA copy number in real-time PCR enables clinicians to investigate how DNA copy number has varied along the clinical course. It

Author Affiliations:
Department of Ophthalmology,
Kinki University School of
Medicine, Osaka-Sayama,
Japan.

also helps to distinguish the ocular flora from the causative pathogens. Thus, appropriate management of corneal ulcers can be achieved in a prompt fashion. We have previously succeeded in using real-time PCR to detect herpes simplex virus in patients with herpetic keratitis.⁸⁻¹⁰ However, to our knowledge, real-time PCR has not been used for the diagnosis of bacterial and fungal keratitis. We there-

fore used 2 methods, microbial culture and Cycleave PCR, to detect and quantitate the causative pathogens in bacterial and fungal ulcers. We assessed and compared the performance of both methods and aimed to determine the clinical potential of Cycleave PCR as a diagnostic tool for corneal ulcer.

METHODS

SUBJECTS AND SAMPLE COLLECTION

We examined 40 eyes of 40 patients (mean age, 51.6 years; range, 16-89 years) who were diagnosed with corneal ulcer between November 2006 and January 2009. All the patients except 1 (case 10) were pretreated with antibiotics before coming to our clinic, Kinki University Hospital. This study adhered to the tenets of the Declaration of Helsinki. All the patients agreed to participate in this study and informed consent was obtained.

Subjects were under local anesthesia by oxybuprocaine eye drops, 0.4%, and an eye speculum was put on before sampling. Two samples were collected from each patient for culture, smear examination, and real-time PCR by corneal scraping. All sterile precautions were taken to avoid contamination during sample collection.⁶ A stainless-steel blade (disposable scalpel No. 15; Feather Safety Razor Co LTD, Gifu, Japan) was used to scrape the lesion. One of the samples was transferred onto the culture media and slide glass with a cotton swab. The smear on the slide glass was examined by gram staining at the Department of Bacteriologic Examination, Kinki University Hospital.

BACTERIAL AND FUNGAL CULTURE

The samples were cultured on blood agar medium (Nissui Pharmaceutical Co Ltd, Tokyo, Japan), chocolate agar medium

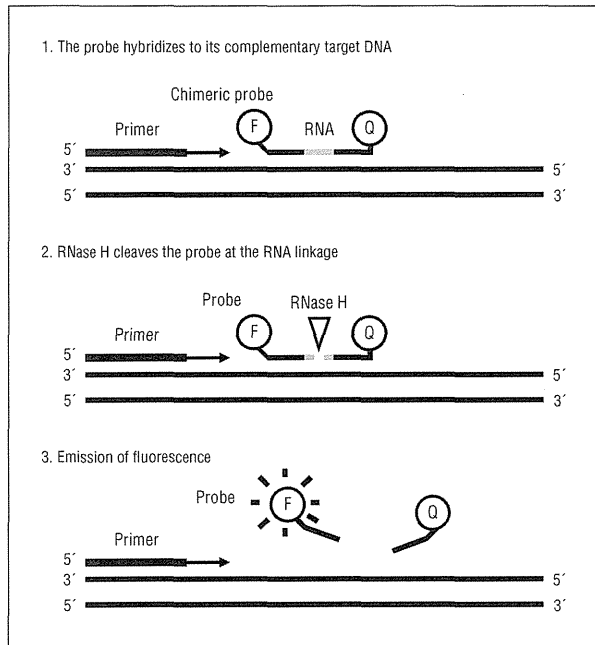


Figure. The principle of the cycling probe technology. F indicates fluorescence; Q, quencher.

Table 1. Primers and Probes Used in Real-Time PCR

Species	Sequence	Target Gene	Size, bp
<i>Staphylococcus aureus</i>		<i>Cap5G</i> and <i>Cap8G</i>	141
Forward	5'-CAACAATACATTTTAGTATCTG-3'		
Reverse	5'-CCAACCTCTTGGATGCGTTG-3'		
Probe	FAM-AT(G)ATATTGCC-Eclipse		
MRSA		<i>mecA</i>	106
Forward	5'-TAACATTGATCGCAACGTTTC-3'		
Reverse	5'-GCTTTGGTCTTTCTGCATTC-3'		
Probe	FAM-TG(G)GATCATAGC-Eclipse		
<i>Staphylococcus pneumoniae</i>		<i>LytA</i>	319
Forward	Not officially published by Takara Bio Inc ^a		
Reverse	Not officially published by Takara Bio Inc		
Probe	Not officially published by Takara Bio Inc		
<i>Pseudomonas aeruginosa</i>		<i>gyrB</i>	120
Forward	5'-CGGAGACCTTCAGCAACA-3'		
Reverse	5'-CGCAGCAGGATGCCGAC-3'		
Probe	FAM-CCTCCTCA(A)CT-Eclipse		
<i>Candida</i> species		<i>ITS2</i>	120
Forward	5'-TGGGTTTGGTGTGAGCA-3'		
Reverse	5'-CAAGCAATGTTTTTGGTTAG-3'		
Probe	FAM-AAT(G)GCTTAGGT-Eclipse		
<i>Fusarium</i> species		<i>EF1-alpha</i>	140
Forward	5'-ACCGACTCAACAATAGGAAG-3'		
Reverse	5'-GTGACAGCGACATACCAATG-3'		
Probe	FAM-GAC(A)AGCTCAAG-Eclipse		

Abbreviations: Eclipse, Eclipse Quencher dye (Epoch Biosciences, Bothell, Washington); FAM, 6-carboxyfluorecein; MRSA, methicillin-resistant *Staphylococcus aureus*; PCR, polymerase chain reaction.

^aTakara Bio Inc (Shiga, Japan).

Table 2. Sensitivities for the 6 Pathogens Detected by Real-Time PCR

DNA Copy No.	Threshold Cycle					
	<i>Staphylococcus aureus</i>	MRSA	<i>Staphylococcus pneumoniae</i>	<i>Pseudomonas aeruginosa</i>	<i>Candida species</i>	<i>Fusarium species</i>
10 ⁶	18.62	19.72	18.33	19.42	17.70	20.41
10 ⁵	21.85	24.03	21.20	22.16	20.55	23.84
10 ⁴	25.47	26.17	24.29	25.48	23.86	26.91
10 ³	28.45	29.78	27.14	28.35	27.04	30.28
10 ²	32.17	33.01	31.30	30.30	29.83	33.44
10 ¹	35.31	37.18	33.35	33.20	33.30	36.14

Abbreviations: MRSA, methicillin-resistant *Staphylococcus aureus*; PCR, polymerase chain reaction.

(Biomerieux Japan, Tokyo), or bromthymol blue glucose agar medium (Biomerieux Japan). If fungal species including *Candida* species and *Fusarium* species were suspected, *Candida* medium EX (Nissui Pharmaceutical Co, Ltd) and Sabouraud agar were used, respectively.

DNA EXTRACTION

The other corneal scraping for real-time PCR was placed into a sterile microcentrifuge tube that included 500 µL of saline solution. DNA was extracted from a corneal scraping specimen using EXTARGEN2 (Tosoh, Tokyo) according to the manufacturer's protocol. Briefly, we first added 100 µL of reagent and 2 µL of detergent for DNA coprecipitation in the tube, and the mixture was vortexed for 5 seconds. Subsequently, 500 µL of protein-denaturing detergent containing 60% (volume to volume ratio) isopropanol was added and the solution was vortexed again for 10 seconds, followed by a 3-minute centrifugation at a speed of 6000 × g. After the supernatant was removed, the precipitate was added to 200 µL of 40% (volume to volume ratio) isopropanol and was vortexed and centrifuged as described earlier. It was then added to 500 µL of 70% ethanol and was vortexed and centrifuged again. Finally, after adding DNase- and RNase-free water to the harvested DNA pellet, the DNA sample was prepared. With this kit, the DNA extraction was completed in approximately 20 minutes.

REAL-TIME PCR

The primers and probes used for Cycleave PCR in this study were designed to simultaneously detect the following 6 pathogens: *Staphylococcus aureus*, *Streptococcus pneumoniae*, *Pseudomonas aeruginosa*, methicillin-resistant *S aureus*, *Candida* species, and *Fusarium* species (**Table 1**). The selected target genes for the specific pathogens were *Cap5G* (GeneBank U81973) and *Cap8G* (GeneBank U73374) for *S aureus*,²¹ *LytA* (Takara Bio Inc) for *S pneumoniae*, *gyrB* (GeneBank EF064840.1) for *P aeruginosa*,²² *mecA* (GeneBank X52593) for methicillin-resistant *S aureus*,^{23,24} *ITS2* (GeneBank ABO32174) for *Candida* species,²⁵ and *EF1-alpha* (GeneBank DQ247583) for *Fusarium* species.²⁶ All the probes were labeled with a 6-carboxyfluorecein reporter dye at the 5' end and with an Eclipse Quencher dye (Epoch Biosciences, Bothell, Washington) at the 3' end. We bought the primers and probe for *S pneumoniae* from Takara Bio Inc. However, the company has not officially published the sequence of these primers and probe.

The real-time PCR assay used 2 × Cycleave PCR reaction mixture (Takara Bio Inc). The reaction mixture contained 20 µL of PCR Master Mix (Takara Bio Inc), 20µM primer, 5µM probe, and 5 µL of DNA sample. The final volume of the reaction mixture was adjusted to 25 µL. The PCR assay was carried out on an ABI PRISM 7000 Sequence Detector (Applied Biosystems,

Table 3. Results of Pathogen Detection by Real-Time PCR and Culture in 39 Cases^a

Real-time PCR ^b result		Culture Result	
		+	-
Bacterial	+	17 (1-17)	9 (24-32)
	-	2 (22-23) ^c	6 ^d
Fungal	+	3 (18-20)	2 (33-34)
	-	0	6 ^d

Abbreviations: MRSA, methicillin-resistant *Staphylococcus aureus*; PCR, polymerase chain reaction; +, positive, -, negative.

^aOf the 40 cases, we excluded case 21 in which *Acanthamoeba* was detected. Numbers in parentheses are the case numbers listed in Tables 4 and 5.

^bReal-time PCR was designed to detect *Staphylococci*, *Staphylococcus pneumoniae*, *Pseudomonas aeruginosa*, *Candida* species, *Fusarium* species, and MRSA.

^cIn the 2 cases with positive culture results only, the detected pathogens (*Staphylococcus warneri* and *Corynebacterium* species) were not included in the 6 target pathogens.

^dSix cases had negative results by both methods that were not distinguishable between bacterial and fungal pathogens.

Foster City, California). The cycling conditions were 10 seconds at 95°C followed by 40 cycles of 10 seconds at 95°C, 10 seconds at 55°C, and 31 seconds at 72°C. The PCR assay was finished in about 2 hours.

The sensitivities for the 6 target pathogens were analyzed using the stock cultures from our laboratory. A standard curve of threshold cycle with values obtained using positive controls was constructed with an established linear range from 1.0 × 10¹ to 1.0 × 10⁶ copies per 25 µL of reaction tube (**Table 2**). Quantification of serially diluted DNA sample was performed by ABI PRISM Sequence Detector software version 1.0 (Applied Biosystems).

COMPARISON OF RESULTS BY CULTURE AND REAL-TIME PCR ASSAY

Culture results after 48 hours were compared with the detected pathogens and DNA copy number obtained by real-time PCR.

RESULTS

PATHOGEN DETECTION BY CULTURE AND REAL-TIME PCR

Of the 40 eyes, Cycleave PCR and culture showed positive results in 32 eyes (80.0%) and 23 eyes (57.5%), respectively (**Tables 3, 4, and 5**). Results of both meth-